The International Journal of Advanced Manufacturing Technology (2022) 120:7707–7720
https://doi.org/10.1007/s00170-022-09274-1

ORIGINAL ARTICLE

Process-related characteristic–based topography evaluation of wear conditions on grinding wheels

Maikel Strug[1] · Berend Denkena[1] · Bernd Breidenstein[1] · Alexander Krödel-Worbes[1]

Received: 15 October 2021 / Accepted: 25 April 2022 / Published online: 3 May 2022

Abstract
Non-productive auxiliary processes affect the single part and small badge production of milling tools. The key production process grinding is inevitably linked to the auxiliary conditioning process. The time demand of those process steps decreases the overall productivity of the manufacturing process. However, today the machine operator decides on conditioning cycles individually by the use of experience. Until today, there is no objective data based approach available that supports the initiation of these conditioning processes or the adaption of the grinding process itself in order to improve its process efficiency. For this purpose, a process-related topography evaluation method of the grinding wheel surface is developed within this study. For the measurement, an optical method based on laser triangulation is used. The measurement system is implemented into a common tool grinding machine tool. In addition, characteristic topography values are defined that show the wear conditions of the grinding tool. Moreover, the data is summarized in a database of wear conditions. The developed measurement method can save grinding and dressing tool resources, process times and minimizes scrap parts. In addition, an adaptation of the process and a targeted launch of auxiliary processes can be enabled. The novel characteristic-based topography measurement creates the opportunity to enhance the tool life of the grinding wheels up to 30% without losing productivity.

Keywords Grinding · Tool wear · Tool condition monitoring · Diamond tools

1 Introduction

An objective approach to setting up grinding processes based on 3D topography parameters of the grinding wheel does not exist to this day. Furthermore, there is no process-related topography evaluation of the grinding wheel surface in order to be able to select the optimal process control variables [1, 2, 5].

In industrial practice, the assessment of whether a grinding tool needs to be dressed usually only takes place indirectly by determining the geometric quality of the ground workpiece. A measurement of the grinding tools is not carried out due to the difficult implementation of an in situ measurement of the grinding wheels. High mechanical and thermal loads on the used grinding tools characterize the tool grinding process itself. The high hardness, the wear resistance, and the low ductility of the cemented carbide to be machined in tool grinding determine the machinability of solid carbide milling and drilling tools, so that diamond grinding wheels are commonly used for machining [2, 6, 7]. A milling or drilling tool mostly is manufactured in the first step by grinding flutes in a peripheral grinding process with a 1A1 grinding wheel (grit size D91–D151; concentration C75–C150). This process is characterized by a high level of engagement and causes high wear on the grinding tools [3, 8, 9]. The following four wear mechanisms occur during grinding: grain flattening or blunting, grain chipping, grain breakage, and chip space clogging. Due to the twisted groove geometry of common end mills and the process kinematics required to manufacture these geometries, the local material removal rate varies significantly along the width of the grinding wheel [3, 4, 10]. This variation leads to locally different types of wear on the grinding wheel. Resin-bonded grinding wheels are often used when machining milling tools. The low thermal stability of the synthetic resin bond in connection with the high thermal conductivity of the diamonds and the strongly fluctuating process loads can lead to an embrittlement of the bond and consequently to the breakage of grains [2].

✉ Maikel Strug
strug@ifw.uni-hannover.de

[1] Institute for Production Engineering and Machine Tools (IFW), Garbsen, Germany

Due to the wide range of wear mechanisms during grinding, there have been studies for over 50 years that aim to evaluate grinding wheel surfaces using measurement technology. In the 1960s and 70 s, measurement methods were used to indirectly assess the condition of the grinding wheel on a macroscopic level. For example, the chip spaces of grinding wheels were examined qualitatively for clogging. The operating principles used are mechanical, pneumatic, electromagnetic, inductive, optical, or acoustic [2, 11, 12]. The interpretation of the measurement signals determined in this way requires much experience in any case, since the measurement methods do not output absolute values, but can only be viewed in relation to one another. In the 1980s, measurement processes for the description of the micro-geometry of grinding wheels were established. These include the tactile profile method as well as optical methods such as confocal microscopy and laser triangulation. The disadvantage of the confocal microscopy method is the low measuring speed. The tools can only be recorded and analyzed over a large area with relatively high amounts of time [2, 4, 13]. Werner's measurements were carried out with a point laser beam in the circumferential direction of the grinding wheel. However, the lack of computational technology limited the investigation of larger areas of the tool. Zitt and Braun, who used a laser triangulation sensor with two receiving modules, made an extension of Werner's method in 1999. This made it possible to reduce shadowing of the laser beam and gaps in the measured profile [14]. After comparing tactile measurement technology and laser triangulation, they came to the conclusion that the optically determined measurement values are influenced by cooling lubricant, but the technology is basically suitable for evaluating wear and checking the dressing result. However, the measuring method could not be transferred to industrial application, as its use in the machining area of a grinding machine is only possible to a limited extent.

2 Experimental setup

This chapter describes the setup for grinding to continually generate wear at the grinding wheel topography. For the setup, a Walter Helitronic Vision 400 L grinding machine tool is used. Metal-bonded grinding wheels were examined (Table 1). The grain size investigated was between 54 and 126 µm; the form was 1A1 with a diameter of 100 mm and a width of 10 mm.

The examined splintery-shaped diamond grains did not show any special features or characteristics and thus represent the standard grain body for the experiments. For the experimental procedure, flat grinding was chosen as an analogy experiment. The material used is CKI®10 with a hardness of 1930 HV30. The cooling is done with SintoGrind

Table 1 Processed grinding wheels

Specification	Bond	Grain size [µm]	Grain concentration
A	Metal	D54	C100
B	Metal	D64	C100
C	Metal	D71	C100
D	Metal	D91	C100

MP 830. The flat grinding process is intended to generate different types of wear at the grinding wheel. The used grinding wheels in shape 1A1 are also used for the production of milling cutters. The grinding of the flanks during the rotation of the blank represents a process structure comparable to flat grinding. Grain wear begins in the crystal layers and is microscopic so that the resolution of measuring laser used can be fully exploited. Typical wear mechanisms of diamond grains are splintering or abrasive wear of the grain edges that can be detected up to an angle drop of 60°, due to the measuring method. Those edges that protrude the highest from the bond and thus reach deepest into the workpiece during processing experience the highest load. Moreover, thermo-mechanical load wears the diamond grains also and lets them appear dull. With the method of laser triangulation, which is introduced later on, only the topography will be measured and no color changes.

In order to generate the wear mechanisms, the flat grinding experiments were carried out by varying the cutting speed v_c, the feed speed v_f and the depth of cut a_e. The material removal rate was continuously adjusted by keeping a constant width (Table 2).

In addition, a maximum force was defined for carrying out the tests, which resulted from machine tool data and grinding wheel data. This force of 500 N must not be exceeded. Otherwise, there is a risk of damage to the tool or the machine (specified by the supplier). In addition, this provides an indicator of when the tests must be terminated and the maximum permissible wear condition of the tools has been reached. In summary, 75 experiments were run in triplicate, which results in a total of 225 experiments. During these tests, the topography measurement using the developed line laser measurement system was carried out between each state of the grinding wheel by starting the measuring

Table 2 Process parameters

Bond	Metal, synthetic resin, vitrified
Cutting speed v_c [m/s]	10, 15, 20, 25
Feed speed v_f [mm/min]	120, 180, 240, 300
Depth of cut a_e [mm]	1, 1.5, 2, 2.5
Width of cut a_p [mm]	5

process after every attempt of grinding. The sequence of these measurements provides a fluctuation for the recording of the grinding wheel topography. In further investigations, these point cloud information will be fed to a process model that is differentiating between cases.

2.1 Development of grinding tool measurement system

In this chapter, the development of a suitable laser triangulation measurement system for grinding wheels and the systems' specifications will be shown. The measuring process will provide a point cloud after the first measurement, which could be processed. The data processing is a planned action for the future research work. It is planned that based on the point cloud information, the grinding process will be adjusted in form of grinding process changes and/or topography adjustments (sharpening, dressing) (Fig. 1).

The laser triangulation sensor used was examined by measuring different grinding wheel topographies with the sensor compared to a tactile measurement system. For the following steps, the Keyence LJ-V 7020 K sensor was chosen. By applying the given measuring parameters (Table 3), a repeat accuracy of 98.5% and a deviation of 1.3% to tactile measurements could be obtained within measuring of a sample size of 336 grinding wheel topographies. The investigation of the necessary measurement parameters took place under laboratory conditions, which were simulated by brightness and environmental adjustments in a shielded box of the machine interior life.

Table 3 Measuring base data

Manufacturer	Keyence
Device	LJ-V7020K
Technology	Optical
Technique	Line scanner, laser triangulation
Measuring time	1 s
Measured surface	15 mm × 6 mm
Point distance	1 µm × 7.5 µm
Trigger-cycle	4 kHz
Binning	Out
Exposure	60 µs
Interpolation	20 points
Sensitivity (1 low, 5 high)	5

However, this type of measurement, as in all optical measurements, is influenced by the topography. Optical processes are limited in their ability to record steep flanks of the measured surface since the emitted light is no longer reflected back to the receiver from a certain flank angle (mostly when

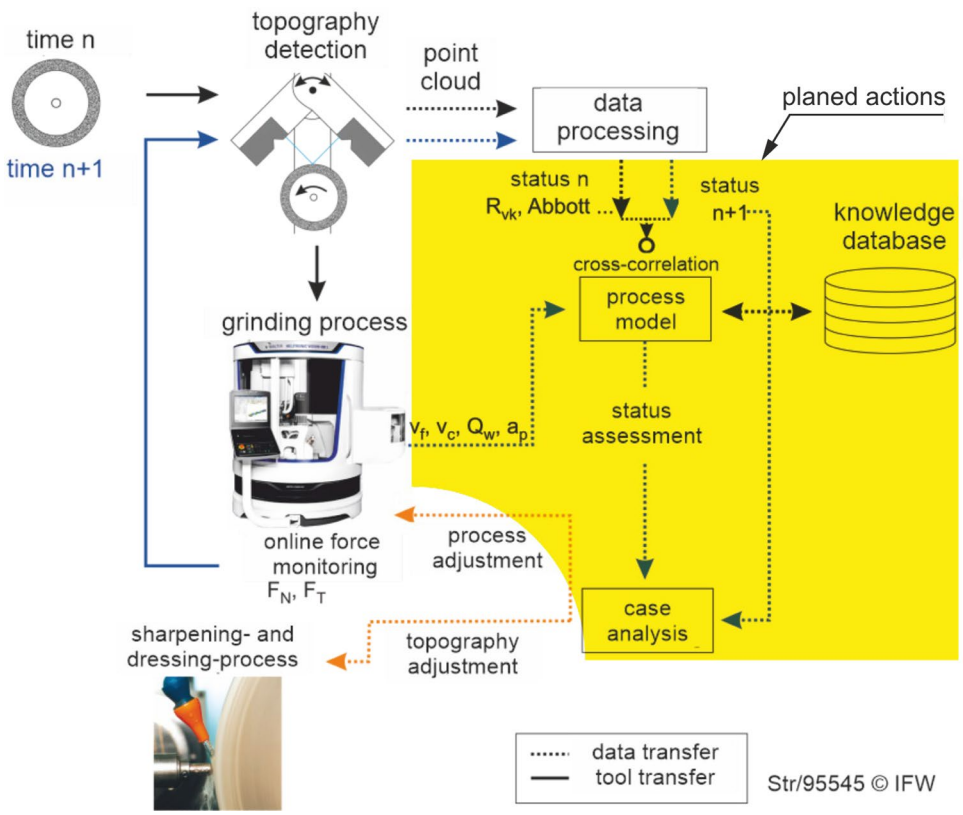

Fig. 1 Experimental measurement procedure

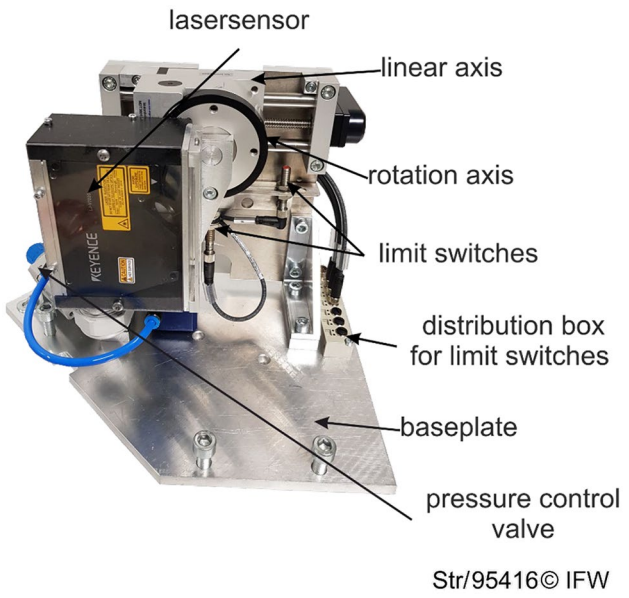

Fig. 2 Measurement system (mount of line scanner)

the angle becomes greater than 60°). Optical measurement systems are limited in measurement accuracy but offer the option of comparably low time-consuming measurements between process steps due to shorter measuring times. Thus this sensor could be implemented in a machine tool. The required accuracy for measuring grinding wheel surfaces is also given here by at least four measured points per grain [2, 4]. It should be noted that when measuring grinding wheels with an average grain diameter of $d_g = 54–126$ µm, the resolution required (54-µm grain leads to a min. point distance of 10 µm, by 800 points to 8 mm) is far below the measurement system's resolution.

This laser sensor is capable to measure sections of grinding wheel surfaces close to the process with the same selected accuracy as other typical measurement systems. With a cycle time of several minutes per grinding cycle, the topography measurement must not exceed a duration of 60 s within the machine in order to be productive [15–17]. This can be achieved with an in-line measurement (Figs. 2 and 3).

The core of the measuring device is a laser triangulation sensor that is embedded in a positioning unit. With the help of this unit, the surface of the grinding wheel can be recorded close to the process. The lower limits for the point spacing in the axial direction of the grinding wheel are 2.5 µm, in the radial direction 0.2 µm and in the circumferential direction 0.5 µm. The sensor in the measuring device can be moved linearly and rotationally. The flexibility is necessary to ensure an adaptation to different grinding wheel diameters (60 to 130 mm). A linear movement supports the realization of the necessary measuring distance, while the

Fig. 3 Measurement system (control unit)

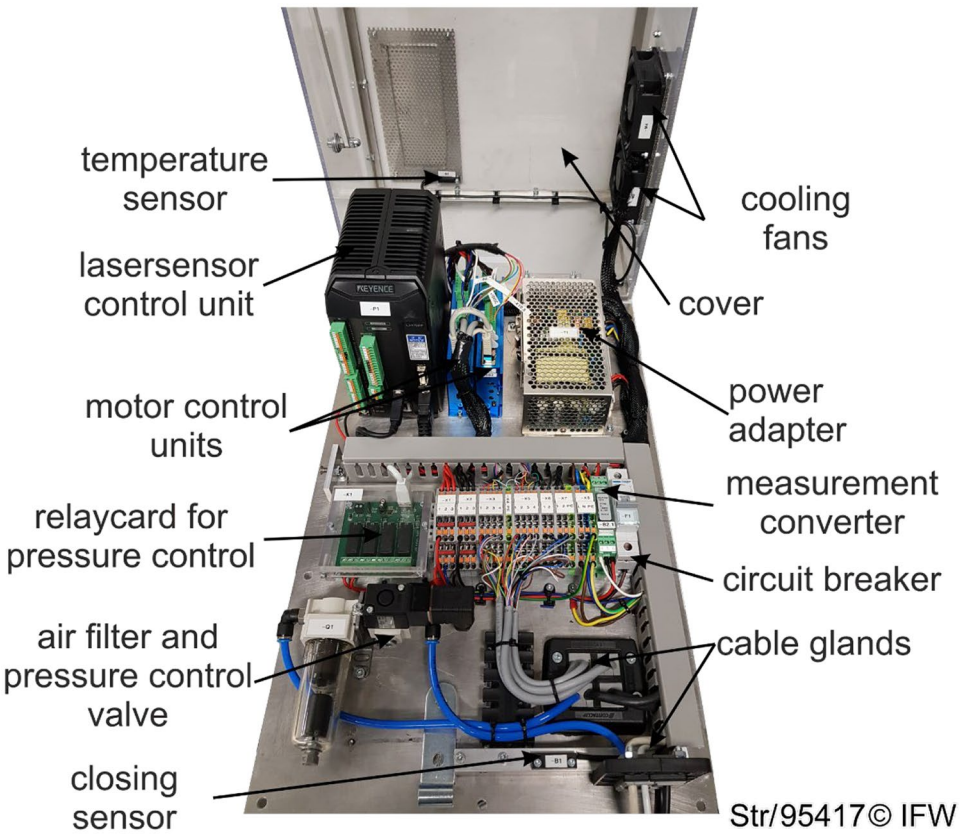

rotary movement enables different angles in relation to the tool surface. Different angles are used for a multiple measurement in case of the unwanted surface reflections leading to mismeasurements. The surface is recorded at an angle of + 15° and − 15°, and the corresponding error points are removed by correlating the surfaces. Both axes are referenced using limit switches that are magnetically controlled (position detection ≤ 1 µm). Overpressure in the sensor housing protects the optical components from external influences such as oil mist. The air supply is regulated separately via a control relay. In addition, the compressed air is cleaned of oils and micro particles by an additional filter. The necessary control elements for these processes are located on a separate control platform that can be retrofitted on the machine in a modular manner (Fig. 2). The complete measurement system is used in a Walter Helitronic Vision 400 L. The measuring device is integrated in the tool changer. The small installation space as well as the risk of contamination by cooling lubricant are restrictions that had to be taken care of for the integration.

For the process of measuring in the machine, an executed NC program positions the grinding wheel near the sensor, which is swiveled into the machine room by means of the tool changer until it has reached the measuring distance of 30 mm. During the measurement, the grinding wheel rotates and the sensor records the surface within a few seconds. For example, the measurement of a grinding wheel with a diameter of 100 mm and a width of 10 mm takes 21 s to measure its entire circumference. The measuring performance is currently 100 mm^2/s. After the measurement, the grinding wheel topography is evaluated. A C-Sharp-based graphical user interface is used to coordinate the axis movements and the measurement of the integrated sensor. For the evaluation and determination of the topography parameters, the measurement uncertainly is targeted in several points. No rounding is carried out in the calculations until the last step, during which the data itself shows a deviation of 1.6% to comparable measurement systems. The repeat accuracy is 98%. With the boundary conditions depicted, a process-related measurement can now be enabled when carrying out wear tests with grinding wheels. Finally, it is worth mentioning that the delay time of the technical components is also taken into account by an implemented waiting time for the axes in order to avoid these small errors.

The evaluated raw measuring data, which is an extract of a metallic grinding wheel experiment, shows a grinding wheel like topography (Fig. 4). Despite the use of unfiltered and thus not processed data, no defects or reflections in the surface can be found. This proofs the theory that measurements of grinding wheels with the laser triangulation sensor are possible and qualitatively sufficient. Moreover, such a closed topography without defects can be used to generate topography values as described in DIN ISO 25178 [18]. The next step is to define different characteristic values that can be technologically linked to the grinding wheel surface. For this consideration, it is important to assign the different parameters to specific properties of the grinding wheel.

The distribution height, function, feature, volume, and hybrid parameters seen in DIN ISO 25178 are not adequate for a grinding tool. Thus, different technological characteristics should be examined. For different wear mechanism to be detected, it is proposed to observe the material volume proportion, the peak height, and the groove depth of the tool surface. This could be depicted by the values S_{pk}, S_{vk},

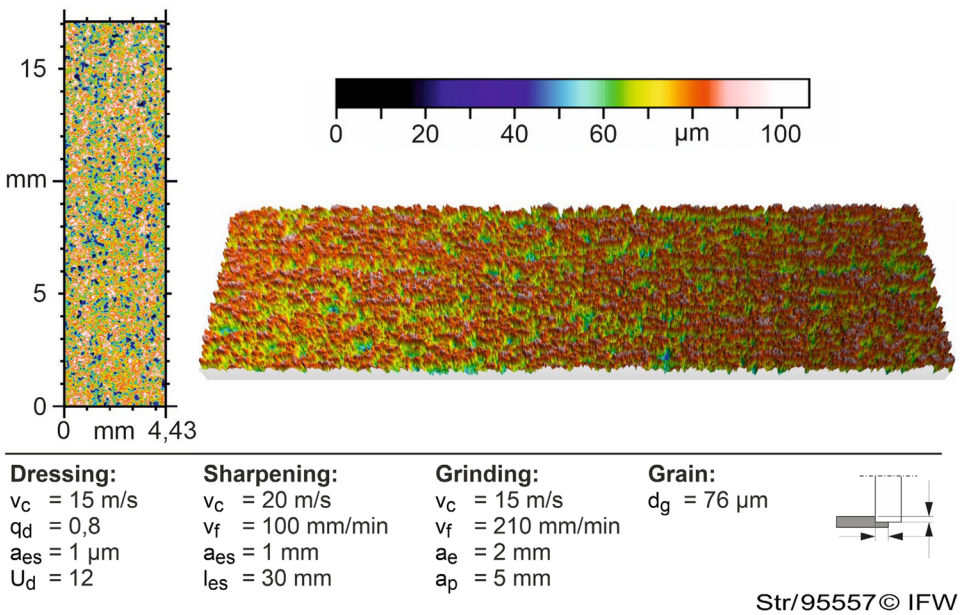

Fig. 4 Raw measuring data (metal bonding, $d_g = 76$ µm)

Table 4 Characteristic values of DIN ISO 25178 to be used for evaluation

Categories of DIN ISO 25178	2D formula sign	3D formula sign	Description	Grinding tool wear attribution
Functional	R_{pk}	S_{pk}	Reduced center height	Grain rounding and break out
	R_{vk}	S_{vk}	Reduced groove depth	Clogging
	M_{r1}/M_{r2}	S_{mr1}/S_{mr2}	Surface material proportion	Grain rounding and break out
Characteristic	-	S_{pc}	Mean value of the tip curvature	Grain rounding
	-	S_{pd}	Peak density	Grain break out
	-	S_{hv}	Volume of a closed hill	Grain rounding and break out
	-	S_{dv}	Volume of a closed valley	Clogging
Volume	-	V_{mp}	Peak material volume	Grain rounding and break out
	-	V_{vv}	Volume of valleys	Clogging

and S_{mr}. Furthermore, mechanisms such as clogging or grain breakouts are also taken into account. This would be possible by mapping the valley volumes or the grain volumes. This leads to the values of the volume of valleys and hills of the topography. In DIN ISO 25178, a distinction is made between closed individual areas and the general volume. For the actual theory, it is preferable to pursue the individual volume of grains S_{hv} and pores S_{dv} similar to the general volume of grains V_{mp} and valleys V_{vv}. Moreover, the grain form should be observed to detect the grain blunting wear. This could be depicted by the value of peak curvature S_{pc}. This enables grains to be distinguished from reflections or defects. Moreover, the grain density is technologically important to observe grain breakouts in a second step or to detect a grain flattening. Thus, the value for peak density S_{pd} will be used. Based on these considerations, the following values are used for the surface evaluation (Table 4).

2.2 In-line measurement of grinding tool topographies

In this chapter, the change of surface parameters over the grinding experiments is examined, and the suitability of the measurement system for the wear evaluation is shown. Thus, the process of flat grinding is used to generate wear at the grinding wheels. The process parameter to be observed is the cutting volume V_w and the related cutting volume $V^{\wedge}_w$.

For the evaluation, the metallic bond is now considered, which is present with diamond grains in different grain sizes (54 µm, 64 µm, 76 µm, and 91 µm). For the comparability of the surfaces, a characteristic grain arrangement is defined and tracked, which is marked in the illustrations (Figs. 5, 6, 7, and 8). This is necessary to ensure an evaluation of the topography compared from one state to the following. This is not necessary for a complete grinding wheel surface evaluation but for surface portions. In this way, areas can be tracked purely optically and local differences can be seen. Moreover, the parameters of the topography are calculated for the complete grinding wheel. A grain rounding can be demonstrated by a decrease in the peak values of the topographies over the course of V_w while the valley structure remains the same (Fig. 5). The absolute peak values, which can be viewed using the S_{xp} value, steadily decrease, which confirms the wear. The change in topography can also be supplemented by an Abbot curve. The slope of the graph at the point of inflection decreases with the main wear of the grain height. The first derivative of the Abbot curve at the inflection point thus forms a decreasing maximum. The decrease in height that occurs here is approximately 50 µm. Other wear mechanisms cannot be clearly identified in these attempts. With this series of measurements, the first wear mechanism can be detected by the developed system.

The wear mechanism of clogging leads to higher peak values in the topography. The valley structure does not remain constant as the material is adhered in valleys of the bond system. The density of valley decreases over the increase of V_w (Fig. 6). Here, pore spaces are clogged, and grains appear taller despite their wear. Moreover, there is a simple method of counting the pores of the topography. If their number decreases, some have been clogged. Furthermore, in Fig. 6, it can be seen that the grain structures remain the same while the valley structures change. With this wear mechanism, the valley structure becomes flatter, and the grains appear larger due to the color resolution. Here, the severity and frequency of the white peaks increases. Despite the lack of distinction between different materials due to the selected measuring method, these mechanisms can be measured with the use of the developed system.

Of course multiple wear mechanism may occur at the same time (Fig. 7). Wear is characterized by locally different characteristics. Rather the progress of wear is different due to the different grain structures and the force load of the process. Thus, Fig. 7 shows how clogging and grain wear increase at the same time but with different intensity. Grains get smaller locally while the valley structure remains the same. On the other hand, valleys and pores become smaller

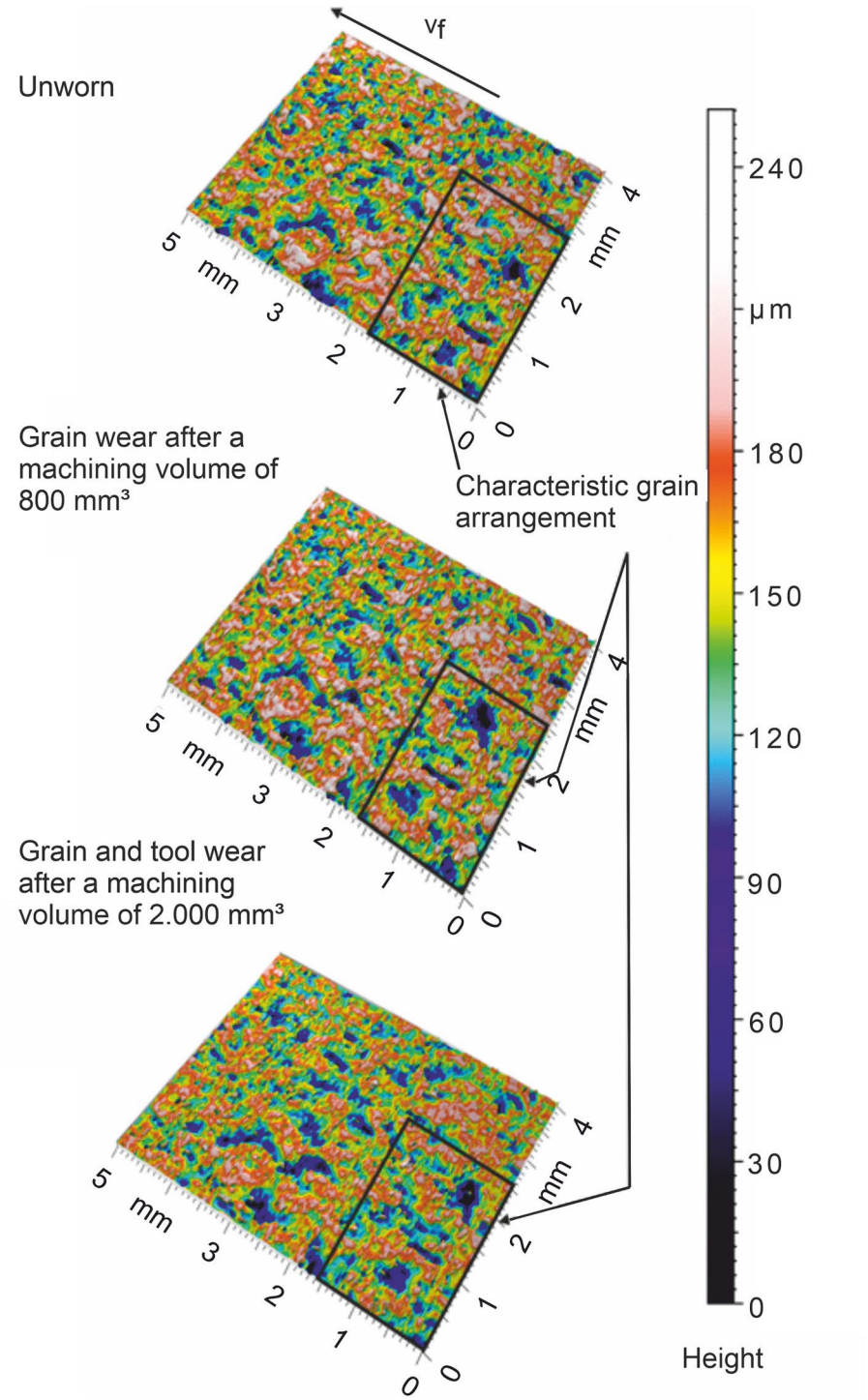

Fig. 5 Tool topographies with grain rounding (top: $V_w = 0$ mm^3, middle: $V_w = 800$ mm^3, bottom: $V_w = 2.000$ mm^3, metal bonding, $d_g = 91$ µm)

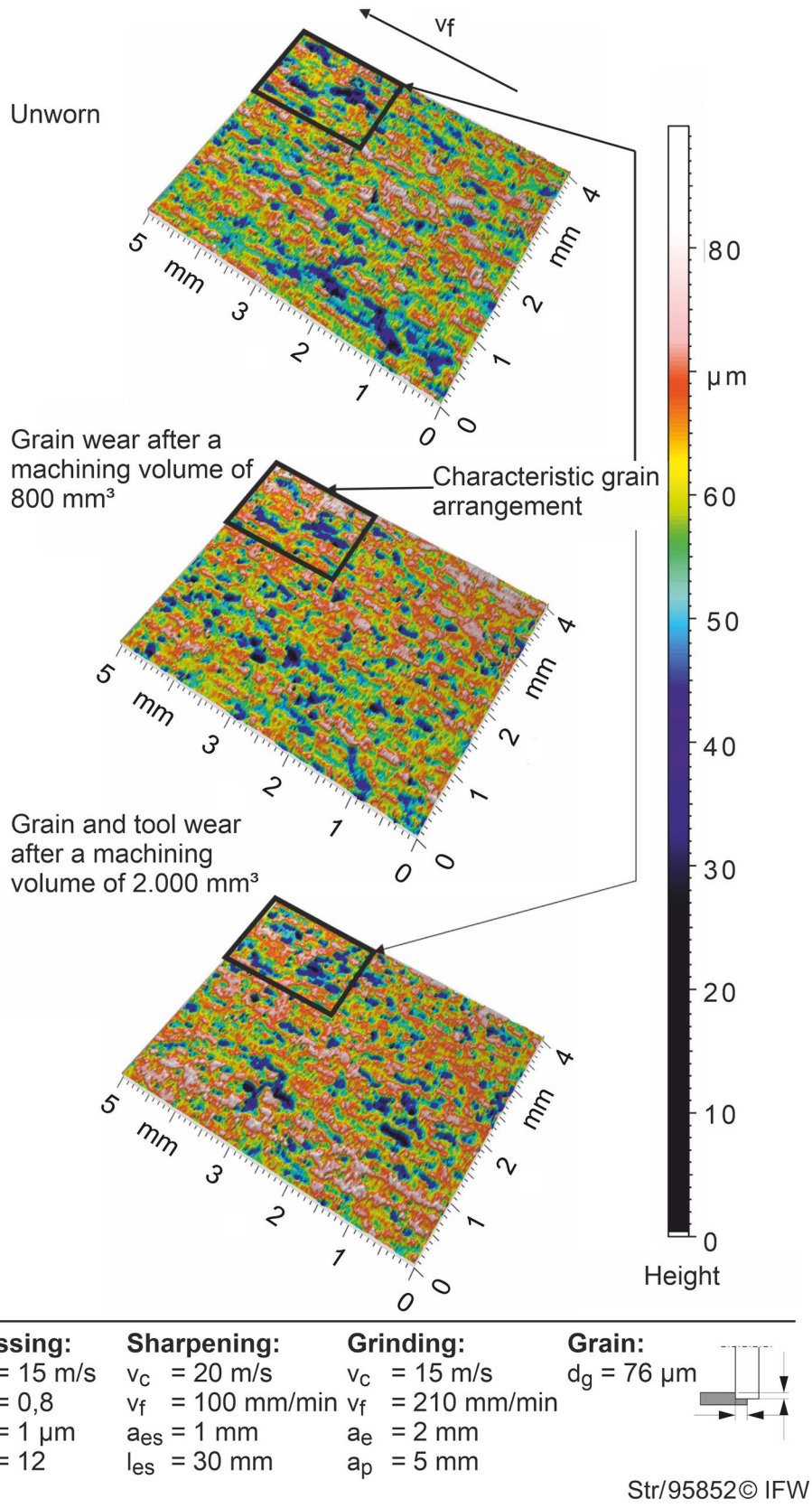

Fig. 6 Tool topographies with clogging (top: $V_w = 0$ mm^3, middle: $V_w = 800$ mm^3, bottom: $V_w = 2.000$ mm^3, metal bonding, $d_g = 76$ µm)

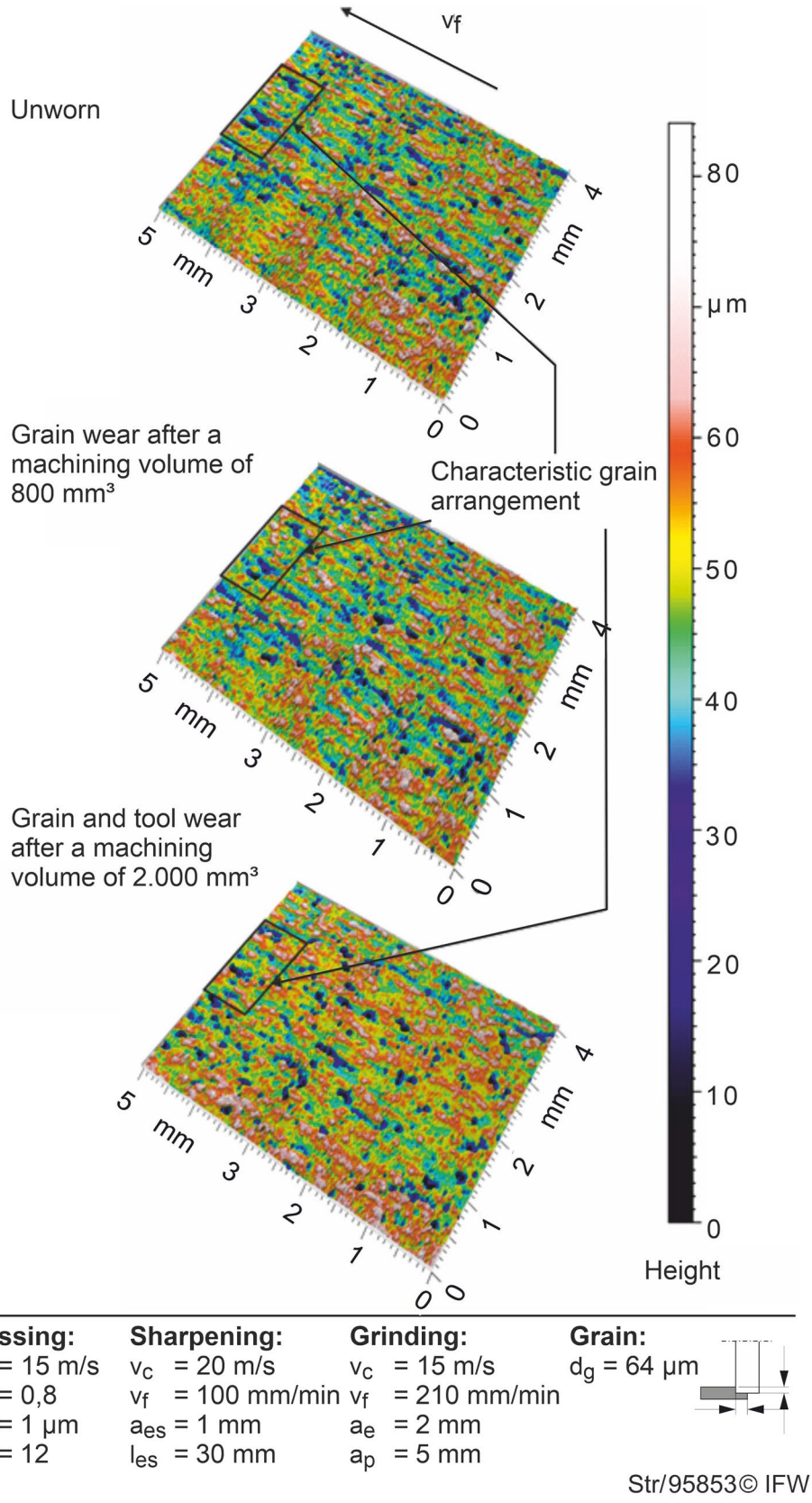

Fig. 7 Tool topographies with grain rounding and clogging (top: $V_w = 0$ mm^3, middle: $V_w = 800$ mm^3, bottom: $V_w = 2.000$ mm^3, metal bonding, $d_g = 64$ µm)

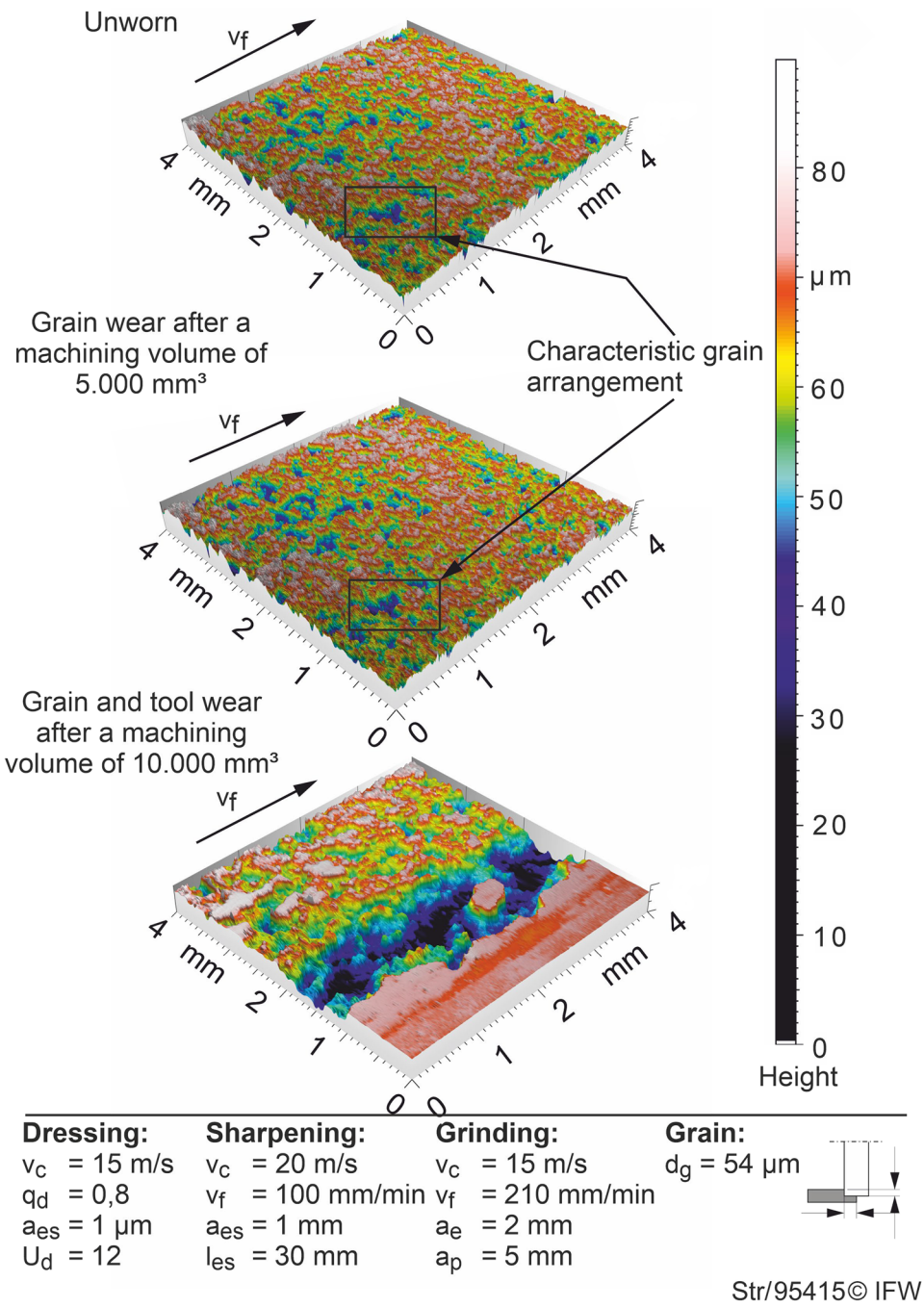

Fig. 8 Tool topographies until severely worn tool (top: $V_w = 0$ mm^3, middle: $V_w = 5.000$ mm^3, bottom: $V_w = 10.000$ mm^3, metal bonding, $d_g = 54$ µm)

or completely flat while the grains appear larger (white) due to the color representation. The grinding wheel is globally worn. Further investigation to increase the wear caused an increase in V_w. This leads to stronger characteristics of the wear phenomena. This ends in overarching clogging, extensive grain breakouts, and a complete flattening of grain structures (Fig. 8). It can be stated that 3D topographies are basically suitable for the detection of grinding wheel wear and that the measuring system used provides topographies that can be evaluated with repeatable accuracy. The next step is to examine the course of the characteristic values and to prove their correlation with the existing wear.

Thus, the different stated surface parameters from the last chapter will be examined. A metal bonding with $d_g = 76$ µm is considered first (Fig. 9). The technological consideration represents that the value S_{pk}, which represents the average height of the grains in the overall topography, should decrease with the increasing tool wear and the grain rounding as well as grain breakouts. This time course is confirmed for the examinations with the grinding wheel. The value of

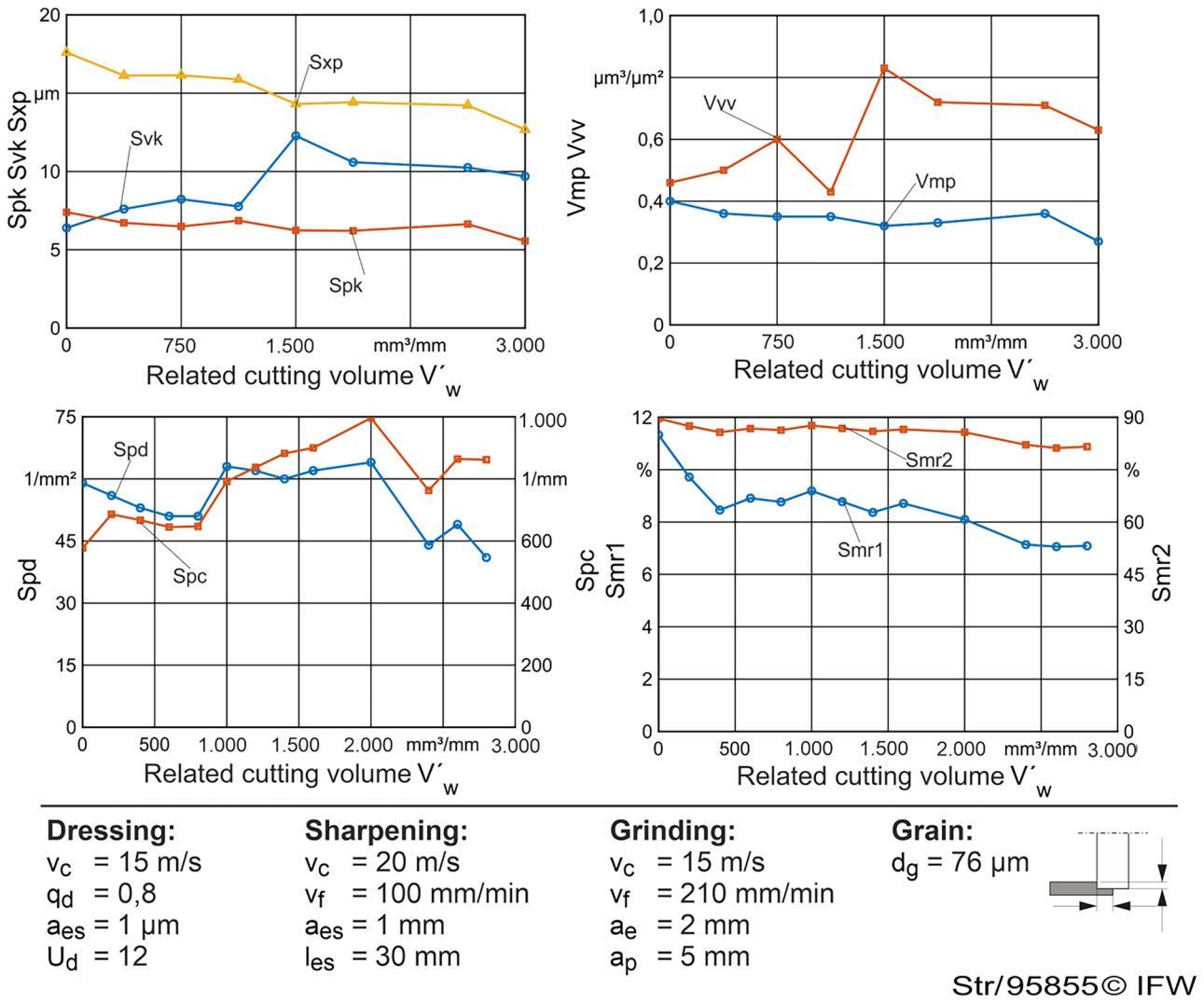

Fig. 9 Characteristic values (top left: S_{pk}, S_{vk}, S_{xp}, top right: V_{mp}, V_{vv}, bottom left: S_{pd}, S_{pc}, bottom right: S_{mr1}, S_{mr2}, metal bonding, $d_g = 76$ µm)

S_{vk} represents the pores and chip spaces. Beside a constant change in grain protrusion, fluctuations are to be expected here due to clogging. For this attempts, the expected development can be detected (Fig. 9, top left). Equivalent attempts were made for all other grinding wheels. For comparison, the metallic bond with a grain size of $d_g = 64$ µm is considered (Fig. 10). The predicted decrease in S_{pk} and the increase in S_{vk} can also be detected here. Technologically, this can be derived and is supported by this result (Fig. 10, top left). The value V_{vv} is now considered further. This represents the volume of the pores and chip spaces. If this value rises above average, there is an increase in volume. Technologically, this can be explained by several grain breakouts or the breakout of the bond. These fluctuations can be detected (Figs. 9 and 10, top right). However, implementation in an automated evaluation algorithm makes this more difficult. Thus, this value is classified as less suitable. On the other hand, the opposite value V_{mp} for the volume of the grains shows the expected decrease over the tool wear. The increasing removal and the rounding of the grains ensure a steady decrease in their volumes. The characteristic value evolves in the same way for all measured grinding wheels (Figs. 9 and 10, top right). Moreover, in further investigations, limit values can be set in order to determine a maximum of grain rounding. The average rounding of the grains is now examined. Thus, the value S_{pc} is detected with increasing tool wear. The peaks of the grain should decrease. Equivalent to other research results, there will be less and flatter grains by increasing tool wear. In this case, the value will increase until the tool is severely worn. Fluctuations of this value can be explained by grain breakouts, as these can lead to valleys with irregular sharp edges. The steady increase of this value can be seen for the different grinding wheels used (Figs. 9 and 10, bottom left). As already noted with the value S_{pc}, the increasing

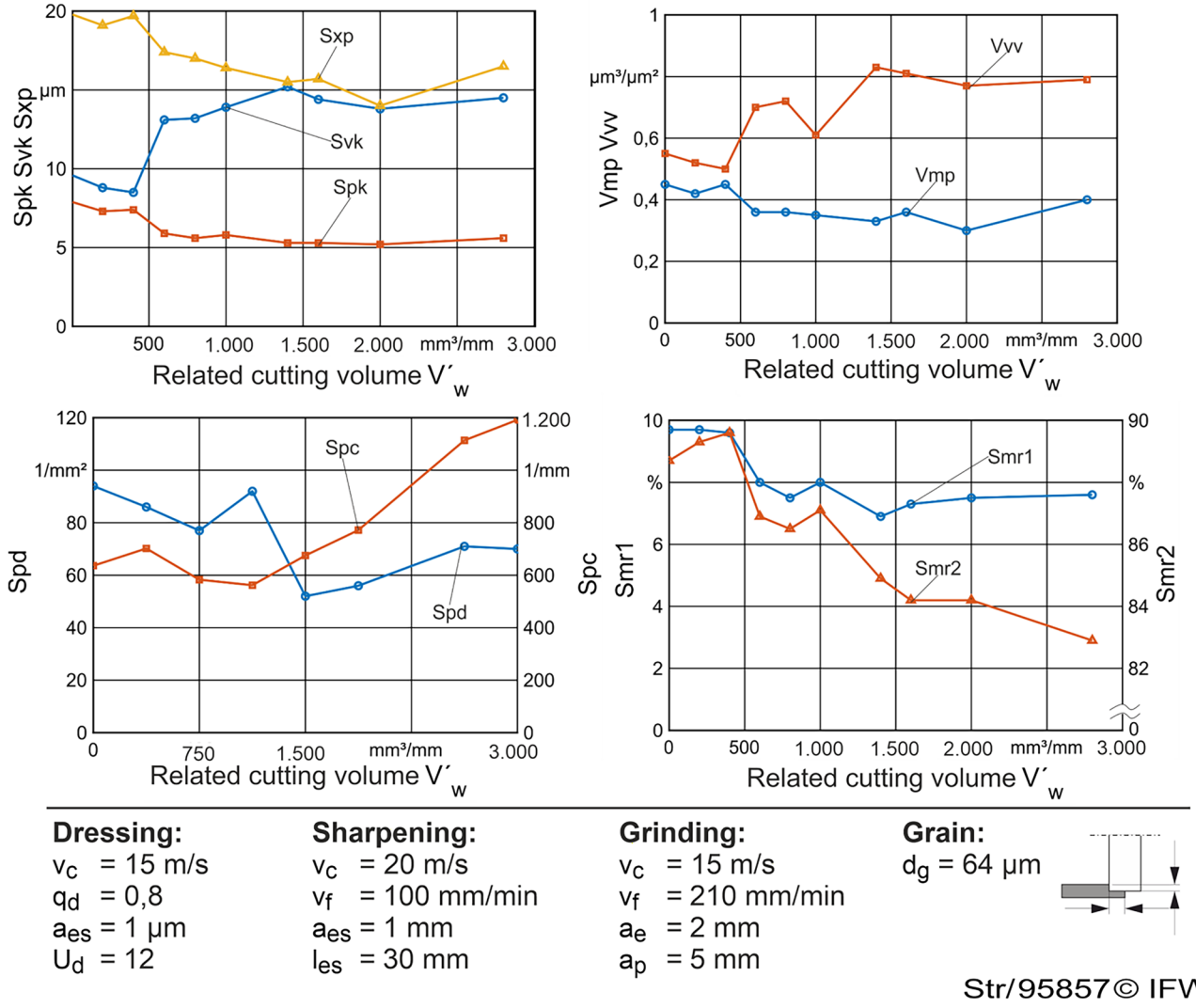

Fig. 10 Characteristic values (top left: S_{pk}, S_{vk}, S_{xp}, top right: V_{mp}, V_{vv}, bottom left: S_{pd}, S_{pc}, bottom right: S_{mr1}, S_{mr2}, metal bonding, $d_g = 64$ µm)

wear of the tools leads to flatter but also less grains. Grain composites are only detected as individual grains and grain break out. This means that the grain density should decrease with wear. This development can be detected for S_{pd}, which represents the density of grains (Figs. 9 and 10, bottom left). Fluctuations for this characteristic value occur as well as for S_{pc} and can be explained equally.

The last characteristic values to be examined are represented by S_{mr1} and S_{mr2}. These represent the material proportion of the peaks and valleys. This is equivalent to the grains on the one hand and to the pores and chip spaces on the other hand. With increasing tool wear, the grains round or break out. This consequently leads to a decrease in material in this area. The material proportion of the valleys is a mathematically inverted value, since this material proportion reflects cavities. These spaces become smaller due to clogging. This leads to a decrease in the proportion of material in the overall grinding wheel topography. From the technological point of view, this means a decrease in both material proportion parameters S_{mr1} and S_{mr2}. The amount of decrease is a measure of the progressive wear of the tool. This course can be confirmed for the investigations under consideration (Figs. 9 and 10, bottom right). The grinding wheels clog and flat areas arise. The development from a grinding process to a friction-like process can be seen. This depends on the increased proportions of friction, which are increasing evenly with the tool wear. This can be further explained by considering the detected process forces (Fig. 11).

The increasing tool wear considered above leads to a flat grinding wheel without chip spaces, pores, or sharp grains. This development can be seen as a grinding process with increased proportions of friction. This ends with a lower roughness at all but results in increasing grinding forces. Thus, the normal and tangential force have been

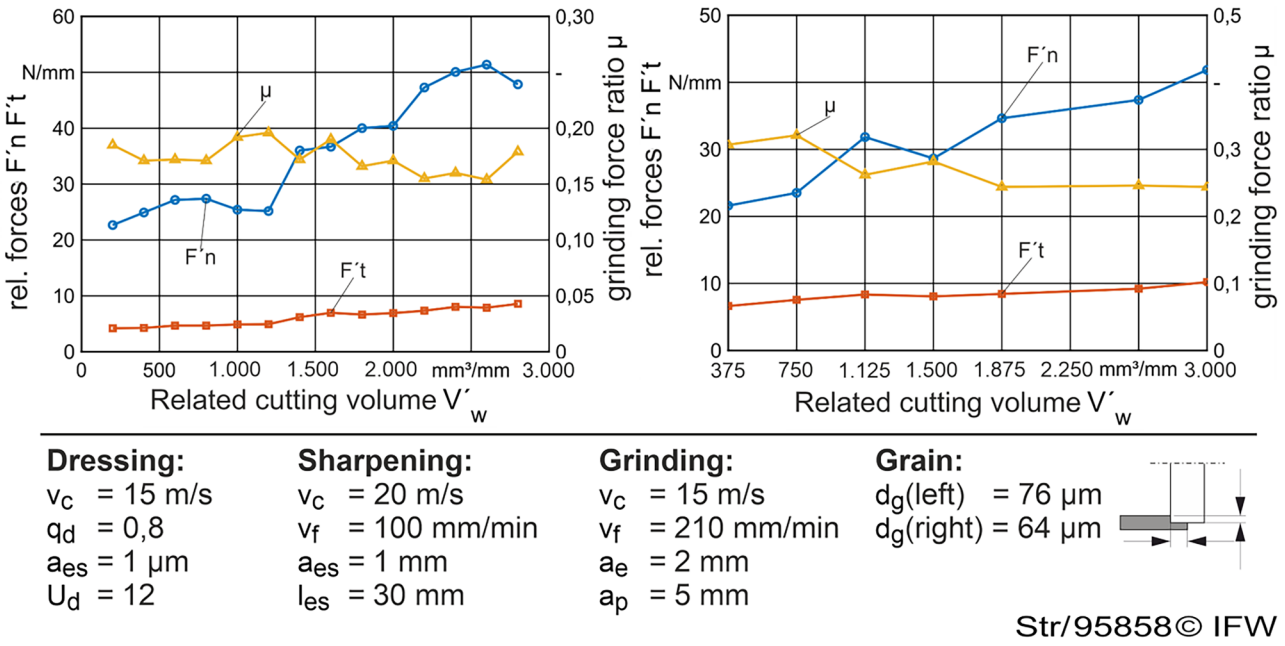

Fig. 11 Measured grinding forces (F'n, F't, μ, left: metal bonding, $d_g = 76$ µm, right: metal bonding, $d_g = 64$ µm)

detected over the hole grinding attempts. The theory states a constant grinding force ratio µ by increasing forces for F_t and F_n. This have been detected for the examined grinding wheels with metal bond (Fig. 11, left $d_g = 76$ µm, right $d_g = 64$ µm).

In summary, the developed measuring system is able to measure wear related topography changes with repeatable accuracy within a machine tool. Of the characteristic values considered, all are suitable for evaluating specific tool wear except for V_{vv}. Overall, the wear characteristics can be sufficiently differentiated. In addition, the changes are large and significant enough for further investigations. This significance of the characteristic values makes it possible to develop and implement algorithms for process control in further steps. A differentiated elaboration using algorithms, divided according to possible process steps like grinding, dressing, and sharpening, must be developed.

3 Conclusion

Wear mechanisms at grinding wheels could be detected by a laser triangulation sensor. Furthermore, the developed and presented measurement system enables process related and efficient topography measurements on grinding wheels, which has not been implemented in this way before. Based on algorithms which will be designed in the next step, an objective and data supported adaptation of the processes will be enabled, so that a reproducible and resource saving process design is feasible. The life cycle of a grinding wheel will be extended while at the same time the costs for non-productive times and the replacement or dressing of a tool decreases. Thus, the often subjective and uneconomical experience of the individual machine operator can be replaced. Based on this, the step towards automating the process can be taken further. Further adjustments will be made in the future, and the entire process will be further optimized for industrial use.

Acknowledgements The authors would like to thank the German Research Foundation (DFG, SFB 653, 5486368) for their organizational and financial support within the project "Characteristic value-based topography assessment and targeted adaptation of grinding processes using self-learning models".

Author contribution Not applicable.

Funding Open Access funding enabled and organized by Projekt DEAL. German Research Foundation.

Availability of data and material Data, NC-code, and materials available on request.

Declarations

Ethics approval Not applicable.

Consent to participate Given by all involved.

Consent for publication Given by all involved.

Competing interests The author declare no competing interests.

References

1. Wiederkehr P, Siebrecht T, Potthoff N (2018) Stochastic modeling of grain wear in geometric physically-based grinding simulations. CIRP Ann Manuf Technol 67:325–328
2. Bergs T, Müller U, Vits F, Barth S (2020) Grinding wheel wear and material removal mechanisms during grinding of polycrystalline diamond. Procedia CIRP, vol 93. New York, p 1.520–1.525
3. Ophey M, Klocke F (2017) Approach for modeling grinding worm wear. International Conference on Gears, International Conference on Gear Production, International Conference on High Performance Plastic Gears, VDI-Verlag. München, p 1.365–1.378
4. Ophey M, Klocke F (2015) Influence of tool specification and machining parameters on the wear behaviour at generating gear grinding. WGP Congress 2015: progress in production engineering. München, p 231–238
5. Hockauf R (2019) Vorhersage spanend gefertigter Bauteiloberflächen. Dissertation, PZH Verlag, Hannover
6. Maldaner J (2008) Verbesserung des Zerspanverhaltens von Werkzeugen mit Hartmetall-Schneidelementen durch Variation der Schleifbearbeitung. Universität Kassel, Dr.-Ing. Diss.
7. Uhlmann E, Schröer N (2015) Advances in tool grinding and development of end mills for machining of fibre reinforced plastics. Procedia CIRP 35:38–44
8. Biermann D, Schumann S, Kansteiner M (2012) Umfassende Betrachtung der mechanischen Belastungen im Schleifprozess. Forum Schneidwerkzeug- und Schleiftechnik, Nr 4(2012):72–83
9. Uhlmann E, Hübert C (2011) Tool grinding of end mill cutting tools made from high performance ceramics and cemented carbides. CIRPAnn Manuf Technol 60:359–362
10. Deichmueller M, Denkena B, de Payrebrune KM, Kröger M, Wiedemann S, Schröder A, Carstensen C (2013) Modeling of process machine interactions in tool grinding. In: Denkena B, Hollmann F (eds) (Hrsg.): Process Machine Interactions. Springer-Verlag, Berlin, p 143–146
11. Karpuschewski B, Inasaki I (2006) Condition monitoring and control for intelligent manufacturing; in: monitoring systems for grinding processes. Springer Verlag
12. Tönshoff H-K, Friemuth T, Becker JC (2002) Process monitoring in grinding. CIRP Ann Manuf Technol 51(2):551–571
13. Klocke F, Wrobel C, Rasim M, Mattfeld P (2016) Approach of characterization of the grinding wheel topography as a contribution to the energy modelling of grinding processes. Procedia CIRP, Bd 46:631–635
14. Zitt U, Braun O (1999) Laser triangulation sensor for the measurement and evaluation of grinding wheel topography within the machine system. Abrasives Magazine, p 24–36
15. Werner F (1995) Anwendung eines Sensorsystems für den Verschleißzustand von Schleifscheiben. Forschungsvereinigung Antriebstechnik, p 98 & 197 & 460
16. Werner F (1994) Hochgeschwindigkeitstriangulation zur Verschleißdiagnose an Schleifwerkzeugen. Dissertation, Universität Hannover
17. Azarhoushang B, Ludwig S (2018) Innovative measurement method to determine the machinability of grinding tools, modern grinding technology and fine machining. 11 edn. Vulkan
18. DIN EN ISO 25178: Geometrische Produktspezifikation - Oberflächenbeschaffenheit: Flächenhaft, DIN Deutsches Institut für Normung e. V.; 2012